ACS APPLIED MATERIALS & INTERFACES

Research Article

www.acsami.org

Electrospray-Processed Soluble Acenes toward the Realization of High-Performance Field-Effect Transistors

Charalampos Pitsalidis,*[,†] Anna-Maria Pappa,[†] Simon Hunter,[‡] Marcia M. Payne,[§] John E. Anthony,[§] Thomas D. Anthopoulos,[‡] and Stergios Logothetidis*[,†]

[†]Laboratory for Thin Films, Nanosystems and Nanometrology, Aristotle University of Thessaloniki, Thessaloniki 54124, Greece

[‡]Blackett Laboratory, Department of Physics and Centre for Plastic Electronics, Imperial College London, London SW7 2AZ, United Kingdom

[§]Department of Chemistry, University of Kentucky, Lexington, Kentucky 40506-0055, United States

Supporting Information

ABSTRACT: Functionalized acenes have proven to be promising compounds in the field of molecular electronics because of their unique features in terms of the stability, performance, and ease of processing. The emerging concept of large-area-compatible techniques for flexible electronics has brought about a wide variety of well-established techniques for the deposition of soluble acenes, with spray-coating representing an especially fruitful approach. In the present study, electrostatic spray deposition is proposed as an alternative to the conventional spray-coating processes, toward the realization of high-performance organic field-effect transistors (OFETs), on both rigid and flexible substrates. Particularly, a thorough study on the effect of the solvent and spraying regime on the resulting crystalline film's morphology is performed. By optimization of the process conditions in terms of control over the size as well as the crystallization scheme of the droplets, desirable morphological features along with high-quality crystal domains are obtained. The fabricated OFETs exhibit excellent electrical characteristics, with high field-effect mobility up to 0.78 $cm^2/(V\ s)$, I_{on}/I_{off} >10^4, and near-zero threshold voltages. Additionally, the good performance of the OFETs realized on plastic substrates gives great potentiality to the proposed method for applications in the challenging field of large-area electronics.

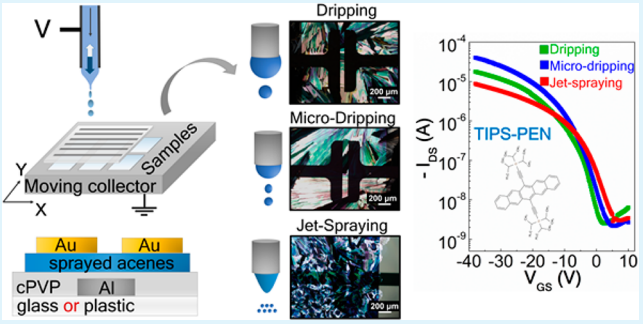

KEYWORDS: *electrostatic spray deposition, organic field-effect transistors, solution processing, soluble acenes, flexible transistors*

1. INTRODUCTION

Organic field-effect transistors (OFETs) have attracted growing interest during the last decades because of their potential to be commercially applied in the next generation of electronic devices.[1−4] Despite the fact that OFETs cannot yet compete with conventional crystalline silicon (Si) transistors, they can outreach the performance of hydrogenated amorphous Si devices, fulfilling the basic requirements for low-cost large-area electronics. One of the main technological challenges in the field of OFETs lies in the development of the active layer. Therefore, the synthesis of novel organic semiconducting materials and/or the ongoing improvement of the manufacturing techniques have already brought about tremendous progress in the device performance.[5−9]

Functionalized acenes, being especially favorable compounds as organic active layers, exhibit good intrinsic field-effect mobilities, enhanced environmental stability, and sufficient solubility in common organic solvents. Among them, triisopropylsilylethynylpentacene (TIPS-PEN)[10] and 2,8-difluoro-5,11-triethylsilylethynylanthradithiophene (diF-TES-ADT)[11] represent two promising organic small molecules with substantial potential because they have reached among the highest charge-carrier mobilities demonstrated so far.[7,12] Several solution-processing methods including drop-casting,[13] spin-coating,[14] blade-coating,[15] and inkjet printing,[16] have been broadly applied for the deposition of organic semiconducting materials, each of them bearing its own advantages over the others. However, none of the aforementioned methods combine the desirable and yet unmet challenges of low material-utilization yield, good control over the deposition process, and compatibility with industrial processes.

Electrospray deposition (ESD), also known as electrohydrodynamic spraying, represents an alternative spray-coating approach toward the formation of thin films over a large area. Specifically, the ESD technique is based on electrohydrodynamic phenomena that occur on the surface of a liquid meniscus, which is ejected through a nozzle by means of a high electric field. Because of the high deposition efficiency,

Received: November 21, 2014
Accepted: March 13, 2015
Published: March 13, 2015

DOI: 10.1021/am508162m
ACS Appl. Mater. Interfaces 2015, 7, 6496−6504

controllability, low-cost processing, and the fact that no gas is needed for atomization of the liquid, ESD is expressly advantageous over conventional spray deposition techniques, rendering it a promising technique in the growing field of organic electronics.[17,18]

In a recent work, Khan et al. fabricated inorganic thin-film transistors using the electrohydrodynamic approach for all the processing steps.[19] Specifically, electrohydrodynamic inkjet printing was applied for the direct patterning of the electrodes, while ESD was incorporated for deposition of the dielectric SiO_2 and the semiconducting ZnO colloidal solution. More recently, Kim et al. reported a study of the ESD conditions required for the deposition of highly conductive poly(3,4-ethylenedioxythiophene)/poly(styrenesulfonate) films toward the fabrication of a top electrode for semitransparent inverted organic solar cells.[20] Interestingly, only a few works have been reported on the application of ESD toward processing of the organic semiconducting layer for field-effect transistors, leaving a wide operating window for process optimization and the investigation of new processing materials. Recently, Onojima et al. reported on the fabrication of bottom-contact TIPS-PEN OFETs using a solvent mixture in order to obtain a stable multijet spraying mode via the ESD method.[21] The resulting devices showed a field-effect mobility of about 0.1 $cm^2/(V\ s)$ and a relatively high threshold voltage. In a more recent attempt, ESD was utilized for the direct patterning of TIPS-PEN and ZnO layers toward the realization of p- and n-type OFETs, with a moderate electrical performance.[22] Thus, despite the interesting capabilities of ESD and the wide range of applicability, further optimization of the process is required in order to improve the performance of the devices and further upscale the method.

In this study, we report on the process optimization of electrosprayed soluble acenes, in order to achieve high-quality crystalline films and further obtain high-performance transistors. Specifically, we performed a detailed study on the effect of the applied voltage on the crystalline formation and overall device performance, in terms of control over the size, transport, and solvent evaporation of the droplets. Moreover, the influence of the solvent properties on the crystallization process was investigated and further correlated with the electrical performance of the devices. The optimized conditions yielded films with well-ordered crystalline structure, while the fabricated OFETs exhibited excellent electrical characteristics. To the best of our knowledge, this is the first systematic study of the crucial variables that determine the crystalline formation of organic semiconducting materials during ESD, toward optimization of OFETs, taking into account both the solution properties and process parameters. It should also be noted that the development of dif-TES-ADT via ESD has not been realized before. Interestingly, the applicability, versatility, and scalability of the proposed method was investigated by the realization of flexible OFETs, which also exhibited especially promising electrical characteristics.

2. EXPERIMENTAL SECTION

2.1. Materials. Triisopropylsilylethynylpentacene (TIPS-PEN) and 2,8-difluoro-5,11-triethylsilylethynylanthradithiophene (diF-TES-ADT) were synthesized in the Center for Applied Energy Research at the University of Kentucky, following the procedure reported elsewhere.[10,11] Poly(vinylphenol) (PVP; M_w = 25 kDa), poly(melamine-*co*-formaldehyde) (PMF; M_n ~ 432, 84 wt % in 1-butanol), propylene glycol methyl ether acetate (PGMEA; >99.5%), tetralin (99.0%, anhydrous), anisole (99.7%, anhydrous), and toluene (99.7%, anhydrous) were purchased from Sigma-Aldrich and used without further purification.

2.2. Sample Preparation. Glass substrates were rinsed with deionized water, ultrasonicated in isopropyl alcohol for 10 min, and left to dry at 120 °C to remove excess solvent. Gate electrodes were formed by depositing aluminum (50 nm) using electron-beam evaporation (0.2 Å/s). A PVP solution (10 wt %) was prepared by adding a cross-linking agent of PMF in a weight ratio of 3:1 in a PGMEA solvent. The PVP dielectric was spun over the prepatterned substrates, followed by thermal annealing at 180 °C for 15 min. The resulting thickness of the dielectric films was approximately 650 nm. For the fabrication of flexible OFETs, heat-stabilized poly(ethylene terephthalate) (PET; Melinex ST504) or poly(ethylene naphthalate) (PEN; Dupont Teonex) was used as the substrate. In this case, the curing temperature for the cross-linking PVP was limited to 160 °C in order to avoid deformation of the substrate. After the development of the dielectric layer onto the substrate, we moved on to deposition of the semiconducting material using the ESD method. Finally, gold source-drain electrodes (50 nm) were vapor-deposited through a shadow mask with various channel lengths and widths in an ultrahigh-vacuum chamber.

2.3. ESD Method. The laboratory setup used in the present work consists of an Esprayer (ES-2000S2, Fuence Co. Ltd.). As seen in Figure 1a, the configuration used in the present setup is "capillary-to-substrate", while the substrate is mounted on a moving collector (motion in the *XY* plane). The patterns of the motion and speed were adjusted using computer software. A constant potential difference was applied between the grounded plate (collector) and a metal capillary (nozzle), through which the solution was pumped at a certain flow rate. In a typical procedure, TIPS-PEN or diF-TES-ADT was dissolved

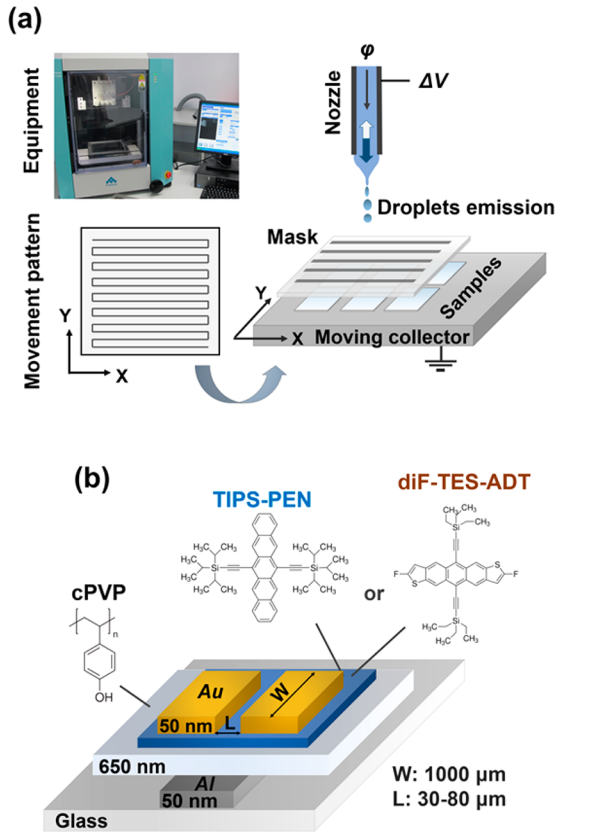

Figure 1. (a) Schematic presentation of the ESD method, laboratory apparatus, and designed pattern used for the collector's movement. ΔV indicates the applied voltage difference between the nozzle and collector, while φ is the flow rate of the solution. (b) Device structure of the fabricated OFETs on glass substrates.

DOI: 10.1021/am508162m
ACS Appl. Mater. Interfaces 2015, 7, 6496−6504

in the appropriate solvent (i.e., tetralin, anisole, and toluene) at a predetermined concentration of 1 wt %. The solution was loaded into a 5 mL glass syringe with a 26-Gauge stainless-steel nozzle. The applied voltage power was in the range of 10−22 kV, while the flow rate was ranging between 0.2 and 2 μL/min. For selective deposition of the semiconductor, a mask was used on top of the samples. The temperature at the collector was fixed at 60 °C, while the distance between the tip of the nozzle and the collector was set at 50 mm. The optimized spraying parameters led to the "microdripping" regime, which was finally applied for the realization of high-performance OFET devices.

2.4. Characterization. For investigation of the surface morphology, atomic force microscopy (AFM) and polarized optical microscopy (POM) measurements were performed via a NTEGRA scanning probe microscope (NT-MDT) and a Nikon LV100, respectively. AFM measurements were conducted in the tapping mode for better image acquisition using rectangular Si cantilevers with 10 nm nominal tip curvature and at a resolution of 512 points/line. In order to determine the crystalline quality of the films, X-ray diffraction (XRD) measurements were performed in the angular range (2θ) of 4−30° with a step size of 0.02°, which is the range where the main reflections of the semiconductors are apparent, via a D-5000 (Bruker) diffractometer with a Cu Kα_1 (2.2 kW X-ray tube) monochromatic radiation source, operating at 40 kV and 40 mA.

Finally, the electrical characteristics of the produced OFETs were investigated using a Keithley 4200SCS semiconductor parameter analyzer under dark and ambient conditions at room temperature. For investigation of the electrical performance, bottom-gate and top-contact OFETs (Figure 1b) incorporating a cross-linked polymeric dielectric were fabricated on glass or plastic substrates. The field-effect mobility values were calculated in the saturation regime from the equation as follows:

$$\mu = \frac{2L}{WC_i}\left(\frac{\partial\sqrt{I_{DS}}}{\partial V_{GS}}\right)^2$$

where W (1000 μm) is the width of the channel, L (30−80 μm) is the length of the channel, C_i is the total measured capacitance per unit area (5.3 nF/cm^2), V_{GS} is the applied gate voltage, and I_{DS} is the drain current.

3. RESULTS AND DISCUSSION

According to the basic principle of electrohydrodynamic spraying processes, the liquid flowing out of a charged capillary nozzle is forced by the electric field to be dispersed into fine droplets. As the surface charge of the liquid reaches a critical value (known as the Rayleigh limit), the electrostatic forces overcome the surface tension and the droplet disrupts into smaller ones in order to reduce the surface charge density by creating more surface area.[23] Particularly in ESD, different operating modes can be observed according to the hydrodynamic phenomena that occur on the electrified liquid meniscus on the capillary nozzle and determine the atomization behavior of the liquid. These phenomena are dependent on a multitude of factors including process variables such as the operating voltage, liquid flow rate, collector-to-nozzle distance, and nozzle diameter as well asinherent solution properties such as the viscosity, surface tension, conductivity, and dielectric constant of the solvent. Changes in the electrohydrodynamic behavior of the liquid result in different spray formation mechanisms (i.e., "dripping", "microdripping", "jet-spraying" modes, etc.) and may yield films with substantially different characteristics. Moreover, in addition to the dominant effect of the spraying regime, the drying behavior of the atomized droplets also defines the characteristics of the resulting film. This is more prominent in the case of crystalline organic semiconductors, where the drying rate strongly defines the overall quality of the films. To this end, TIPS-PEN was utilized in our reference study in order to exploit the effect of the solvent as well as to investigate the optimum spraying parameters that lead to the desired film characteristics for the development of high-performance OFETs.

3.1. Effect of the Solvent on Crystallization of the Droplets. In the ESD process, the solvent properties can dramatically alter the interactions occurring in the electrified pendant drop, rendering the proper choice of solvent crucial, as already stated in several studies.[23,24] As a consequence of the general principles of ESD, the utilization of high relative dielectric constant (ε) solvents and high conductivity liquids easily gives access to the so-called "cone jet-spraying" modes.[25] These modes may be advantageous when smooth and dense films such as the dielectric layers are required because of the establishment of efficient near-monodisperse atomization.[26] However, such a case is not desirable for crystalline semiconductors because miniaturization of the transferred liquid fragments and their subsequent fast evaporation could result in insufficient crystallization and increased grain boundaries. Therefore, we herein investigated the use of low ε solvents in order to bring about a larger optimization window in the process and achieve the desirable electrospraying scheme by varying the spraying parameters. Additionally, the relatively low surface tension values of the solvents used in this work facilitate atomization of the liquid in the operating voltages because too high surface tension could lead to spraying instabilities. Specifically, toluene, anisole, and tetralin, three solvents of considerably different vapor pressure and boiling point, the physical properties of which are shown in Table 1, were electrospray-deposited, and the structural and morphological properties of the resulting films are presented below.

Table 1. Physical Properties of the Solvents Used in This Work

	solvent properties			
solvent	dielectric constant (ε)	surface tension (γ) [dyn/cm]	boiling point [°C]	vapor pressure [kPa] (25 °C)
toluene	2.4	28.8	110.6	3.69
anisole	4.3	29.3	154.0	0.55
tetralin	2.8	35.9	210.3	0.04

Parts a−c in the Figure 2 show the POM images of the three differently dried TIPS-PEN films. Particularly, when a solvent with high vapor pressure (and consequently high evaporation rate), such as toluene (Figure 2a), was used, evaporation took place almost instantaneously, and individual droplets with a ringlike structure marking the periphery line of the droplet were observed. The main characteristic of such a formation is the significant crystal accumulation at the droplet's contact edges, which can be explained by the so-called "coffee-stain" phenomenon. This effect is driven by domination of the convective flow, which causes the solute to be transferred and deposited near the edges. Thus, coalesced crystalline stains characterized by discontinuities and large gaps between the apparent crystalline domains were observed. It should be noted that such defects are known to be charge traps that can potentially induce current resistance at the conducting channel.[27,28] As has been previously argued, the decrease of the solvent evaporation rate can improve the homogeneity of the film, by giving more time for the pinning/depinning of the contact line as well as for the molecules to self-assemble into

DOI: 10.1021/am508162m
ACS Appl. Mater. Interfaces 2015, 7, 6496−6504

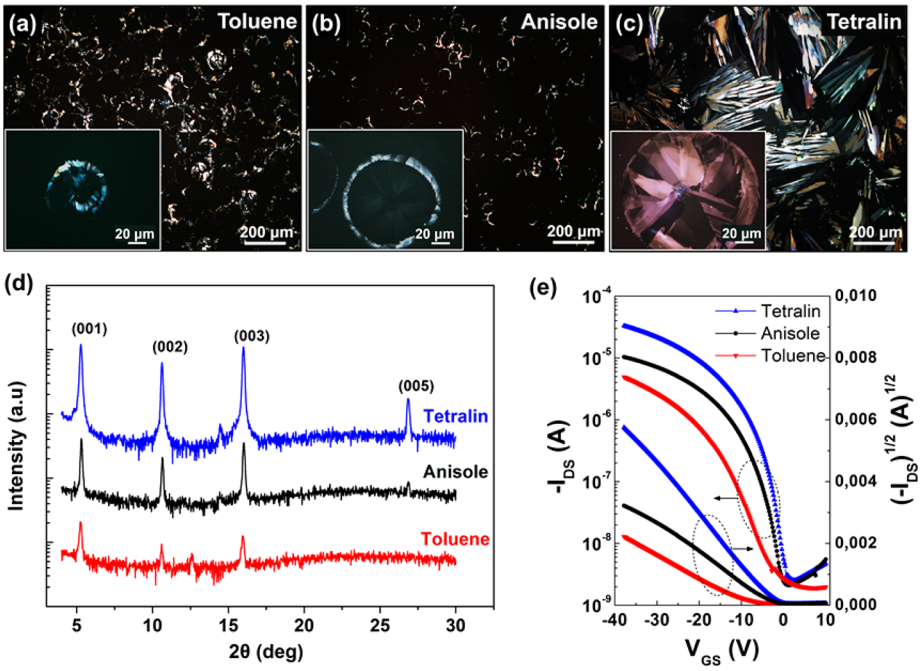

Figure 2. POM images of electrosprayed TIPS-PEN from various solvents: (a) toluene; (b) anisole, ;(c) tetralin. The inset images show the corresponding droplets. (d) Comparative XRD diagram and (e) representative transfer characteristics of TIPS-PEN OFETs electrosprayed from different solvents.

highly ordered structures.[29,30] The above assumption was confirmed when a less volatile solvent such as anisole was used. Evaporation in this case was observed to take place within a few seconds, and as shown in Figure 2b, the morphology of the films was improved, exhibiting a more uniform crystal distribution over the substrate. Even though thin grains were observed to grow radially at the inner regions of the droplet, a thick ring stain still existed, which is evident in the corresponding inset image. In both aforementioned cases, the drying process was relatively fast and crystallization was confined to the volume of each individual droplet, restricting the formation of continuous crystalline domains. Conversely, a substantial improvement in the resulting morphology was observed when tetralin, with 2 orders of magnitude lower vapor pressure than toluene, was applied (Figure 2c). This was attributed to its slow evaporation, which took place within the first few minutes, thus enabling the contiguous droplets to coalesce into larger continuous volumes and self-organize into well-ordered crystalline domains via nucleation and growth. Additionally, the ring stain was nearly absent while the film displayed a more dense crystalline morphology. Conclusively, the solvent with the lower evaporation rate led to the optimum crystalline structures because it provides sufficient time for the crystals to organize into well-defined structures.

To gain a better understanding of variation of the film microstructure, XRD measurements were performed. Figure 2d shows comparative out-of-plane (θ–2θ mode) XRD patterns of the electrospray-deposited films from various solvents. All of the films showed distinct (00l) diffraction peaks, indicating the presence of highly ordered crystal phases even up to fifth order (005). By a comparison of the relative intensities of the spectra, it is clearly supported that the films from tetralin led to more intense peaks, implying the formation of significantly larger and/or better-ordered grains. This fact confirms that the solvent critically deterermines the crystalline quality of the electrosprayed films.

In order to further investigate the above findings, the morphological and structural properties were correlated with the electrical behavior of OFET devices. Figure 2e shows the representative transfer characteristic curves of different OFET devices using various solvents. A distinct difference (almost by a factor of 6.5) was found in the maximum drain current of the transistors, which reflects a strong variation in the field-effect mobility. In these particular OFETs, the extracted mobility was 0.32 cm^2/(V s) in the case of tetralin, while for anisole- and toluene-based OFETs, the mobilities were calculated to be much lower, 0.13 and 0.065 cm^2/(V s), respectively. This performance discrepancy is assigned to the significant differences in the crystalline characteristics of the semiconducting film. In other words, insufficient crystallization and coalescence of contiguous crystalline stains most likely introduced certain defects and local disorders, which disrupted the π–π stacking of the molecules and thus limited charge-carrier transport. Taking into account the above considerations, it is concluded that tetralin exhibited the preferred drying behavior for crystallization of soluble acenes.

3.2. Effect of the Applied Voltage on Droplet Formation. As previously described, ESD exhibits a variety of spraying regimes, the classification of which is based on the morphology and dynamics of the liquid meniscus.[31,32] There are many parameters that interdependently influence the electrohydrodynamic disintegration mechanism of the liquid meniscus and subsequently the electrospraying regime, with the applied voltage and liquid flow rate being considered as the most determining ones.[33] To date, several functioning modes have already been described, with dripping, microdripping, and cone jet spraying being the most commonly studied. This order of succession of modes is often observed in relation to the voltage increase.

In our case, we were able to initiate electrohydrodynamic effects on the pendant droplet after a critical voltage value of around 12 kV, where infrequent disruptions on the droplet

DOI: 10.1021/am508162m
ACS Appl. Mater. Interfaces 2015, 7, 6496–6504

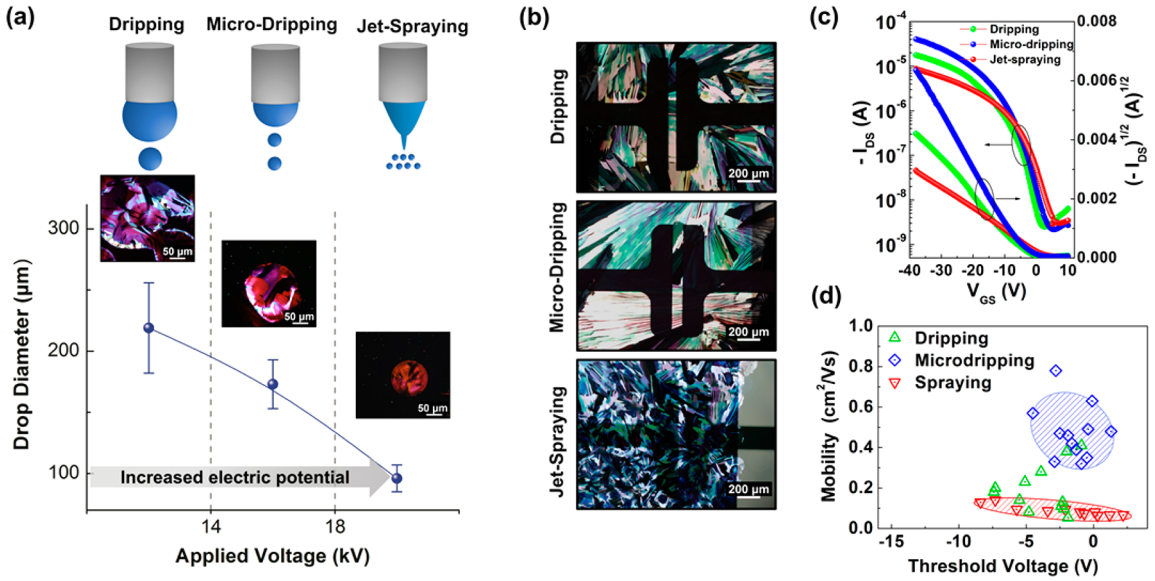

Figure 3. (a) TIPS-PEN droplet size distribution and the corresponding POM images of individual droplets for different spraying regimes. (b) POM images showing crystal formation in the channel region of the transistors. (c) Comparison of typical *I*−*V* transfer characteristics. (d) Device uniformity diagram showing the mobility and corresponding threshold voltage values of the fabricated OFETs with respect to the spraying regime.

surface were observed, resulting in the emission of large-sized droplets. This mode, which can be easily paralleled with a dripping faucet, occurs generally when the voltage is sufficient enough to overcome the liquid surface tension and is characterized by an irregular emission of large droplets.[34] Upon a gradual increase in the capillary voltage, changes in the geometry of the pendant drop can be observed, leading to deformation at the surface of the pendant drop, which results in a frequent emission of droplets, disintegrated from the meniscus of the solution (microdripping mode). Indeed, when higher voltages (14−18 kV) were applied, a regular pulsating emission of droplets was observed, the frequency of which increased with the voltage while the size of the droplets subsequently decreased. Finally, further increasing the voltage (>18 kV) led to a noticeable deformation/extension, forming a jet on the pendant drop and its subsequent breakup into several microdroplets (jet spraying).[31] Therefore, it seems that there is a tendency for the primary emitted droplets to decrease their volume/size with a voltage increase. These observations are consistent with the previously published results on electrohydrodynamic spraying effects.[35] It is essential to add that all of the aforementioned spraying characteristics were obtained by adjusting the flow rate (0.2−2 μL/min) at a given applied voltage. Also, it should be noted that the boundary conditions between the various regimes were qualitatively defined via visual inspection of the spraying process and produced films.

As seen in Figure 3a, each spraying scheme resulted in profoundly different droplet characteristics, such as the size and dispersity (indicated by the error bars in the graphs). As expected, the dripping mode resulted in large and nonuniform-sized droplets of various shapes because of the liquid emission instabilities. Conversely, the stable spraying profile observed in the jet-spraying mode resulted in a more uniform distribution of small droplets (<100 μm). Because the drying behavior of the droplet is strongly influenced by its size/volume, the production of very small droplets is not advantageous in the case of crystalline formation because tiny droplets tend to evaporate too fast and lead to the formation of smaller crystal domains. Consequently, the microdripping regime demonstrated a more balanced condition between the two aforementioned regimes because it combined good control over the droplet size along with efficient crystallization.

The morphology of the differently sprayed crystalline films over the entire device area of the transistor is shown in the POM images of Figure 3b. Additional morphological information regarding the size and shape of the crystals is provided in AFM imaging in Figure S1 in the Supporting Information (SI). As can be seen from morphological analysis, the microdripping regime led to a more uniform and well-distributed group of crystalline domains, contrary to the bulky and highly anisotropic crystals observed in the dripping regime as well as to the smaller crystalline fractions of various shapes and sizes, randomly distributed in the case of the jet-sprayed films.

In order to correlate the above-mentioned characteristics of the fabricated OFETs with their electrical behavior, we performed electrical measurements on the differently sprayed devices. Figure 3c shows a comparative diagram of representative *I*−*V* transfer characteristics for each spraying mode. Despite the satisfactory performance demonstrated in the case of the dripping mode in terms of mobility [μ_{avg}= 0.19 ± 0.12 $cm^2/(V\ s)$], the uncontrollable spraying behavior during this regime, along with the inhomogeneous crystal size and shape, renders it unreliable and with limited applicability. The fabricated transistors via the microdripping regime yielded a superior electrical performance with an average mobility of 0.47 ± 0.13 $cm^2/(V\ s)$, as a result of improved crystalline film morphology. Oppositely, the jet-sprayed films resulted in inferior electrical characteristics with a significantly lower average mobility of 0.086 ± 0.025 $cm^2/(V\ s)$ because of their poor crystalline quality, which seems to have brought about an increased density of grain boundaries along with a non-negligible amount of film defects, resulting in mediocre electrical characteristics.[36] The average mobility and standard deviation values were calculated from 12 different transistors for each spraying regime.

Notably, one of the primary drawbacks faced in large-area solution processing (i.e., spraying) of crystalline semiconduc-

DOI: 10.1021/am508162m
ACS Appl. Mater. Interfaces 2015, 7, 6496−6504

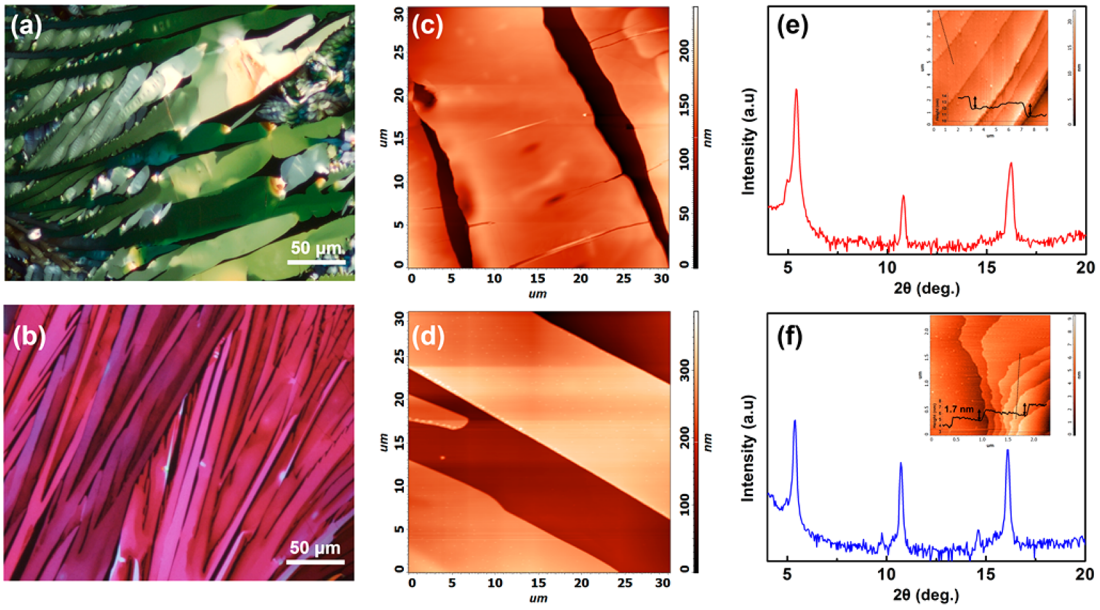

Figure 4. (a and b) POM images, (c and d) AFM topography, and (e and f) out-of-plane XRD patterns of the electrospray-deposited diF-TES-ADT and TIPS-PEN films, respectively. The insets show the AFM topographs of the layered structures and the corresponding height profile.

tors is the lack of evaporation control because it is extremely difficult to restrict random crystalline formation and consequent charge-carrier anisotropy. Figure 3d shows a diagram of the device performance uniformity for each spraying regime used. Specifically, as indicated by the spread of the scatter points, the electrical characteristics of OFETs prepared using the dripping mode are randomly and widely diffused, confirming the uncontrollable behavior of such devices. The mobility values in the jet-spraying scheme, on the other hand, show low device-to-device variations, although the corresponding threshold voltage values appear widely diffused. This is likely attributed to the poor interfacial quality between the semiconductor and insulator. In line with the observed crystalline characteristics, the microdripping mode yielded improved electrical behavior in total, with low threshold voltage (<−4 V) and high mobility values with acceptable distribution.

It is worth noting that there are some additional factors such as the distance and movement of the collector that can also influence the properties of the films. Specifically, in our case, the distance was adjusted in order to compensate for maintaining the shape/size of the droplets while avoiding evaporation before reaching the substrate.[37] Additionally, significant variations in the homogeneity of the sprayed films were observed when the speed of the collector was modified. Precisely, when the speed of the collector's movement (at a constant spraying rate) was too high, films were characterized by poor crystal connectivity, while in the opposite condition, extensive overlapping of the droplets influenced the drying process and led to the establishment of bulky nonuniform crystals. In conclusion, ESD is a dynamic process and its outcome is driven by complex interactions, which are greatly dependent on the interplay between the solute/solvent with the substrate and the applied voltage.

3.3. Morphological and Electrical Characteristics of the Optimized OFETs. Following optimization of the process parameters described above, the TIPS-PEN and dif-TES-ADT films were deposited using the microdripping mode of ESD. The crystalline characteristics of the produced films were investigated by performing structural and morphological analysis by means of POM, XRD, and AFM measurements. Parts a and b in Figure 4 show the POM images of the optimally electrospray-deposited TIPS-PEN and diF-TES-ADT crystals formed on the cross-linked PVP (cPVP)/glass substrates, respectively. The strong and clear optical birefringence under polarized light indicates the well-preserved crystalline nature in the produced films. The slight inconsistency in the brightness and color is related to variation in the thickness and orientation of the crystals. Despite the visible crystalline orientation, it is straightforward that maintaining uniaxially oriented films over a large area under spraying conditions is still challenging because of difficulties in controlling the drying process. As can be observed, TIPS-PEN showed a tendency to crystallize into elongated needlelike crystals, while diF-TES-ADT crystals adopted a platelet-like shape. In Figure 4c,d, we present the representative topographic AFM measurements of the grown crystals. As calculated from the peak-to-valley values, the crystal thicknesses were comparable in both cases, ranging from 120 to 180 nm. Correspondingly, the average width of the crystals was found in the range of 10−40 μm. Such morphological features indicate a highly ordered π stacking within the large crystalline grains, which is typically observed in other evaporation-induced crystallization methods.[38,39] It is worth noting that the surface properties of the substrate may dramatically influence the wetting behavior and resulting crystalline morphology. PVP demonstrated excellent compatibility with both functionalized acenes, providing a suitable surface in terms of roughness, while its relatively low surface energy clearly favored adhesion of the hydrophobic silyl groups and promoted molecular stacking and ordering (see Figure S2 in the SI). This fact was further confirmed by the XRD measurements of the films grown on the PVP layer.

Parts e and f of Figure 4 show the out-of-plane XRD spectra of the diF-TES-ADT and TIPS-PEN films, respectively. Both types of samples exhibited a series of intense (00*l*) peaks, indicating the highly ordered crystalline phase, confirming that the molecules are stacked with their silyl groups on the

DOI: 10.1021/am508162m
ACS Appl. Mater. Interfaces 2015, 7, 6496−6504

substrate surface. According to Bragg's law ($2d \sin \theta = n\lambda$, where λ = 1.54 Å), a d spacing of approximately 16.6 ± 0.2 Å was calculated for the primary peak at 2θ =5.28 ± 0.4°, which was found to match well with the length of the c-axis unit cell of the molecules.[10,11] Further evidence of molecular orientation was provided by the AFM topography (see the insets) of the crystals, which revealed a terracelike surface morphology, implying the layer-by-layer self-structuring of the molecules. The cross-sectional profile between two consecutive layers was found around 1.7 nm, which coincides with the results from XRD analysis. These results suggest that the sprayed films maintain favorable molecular orientation, which benefits efficient charge-carrier transport.

The transfer and output characteristics of the best-performing transistors based on TIPS-PEN and diF-TES-ADT semiconductors are shown in Figure 5. Both types of OFETs

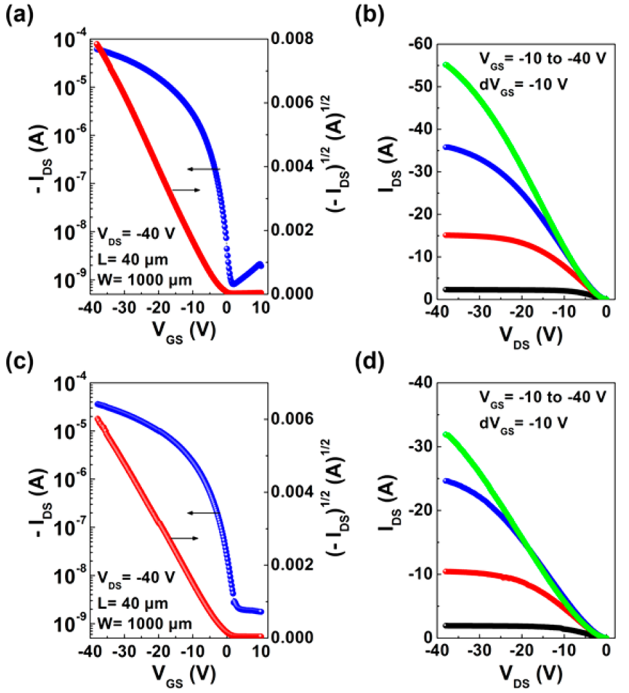

Figure 5. Transfer (I_{DS}–V_{GS}) and output (I_{DS}–V_{DS}) characteristics of the best-performing electrosprayed (a and b) TIPS-PEN and (c and d) diF-TES-ADT OFETs. Devices had a top-contact/bottom-gate geometry, while their channel length and width were 40 and 1000 μm, respectively.

exhibited typical p-type behavior with a distinct turn-on point and a clear transition between linear and saturation regimes. The apparent deviation from linearity at low V_{DS} in the output plots implies the presence of a Schottky-like barrier. This superlinear behavior is most likely attributed to the energy misalignment or morphological effects at the interface between the semiconductor and contacts.[40,41] Table 2 summarizes the electrical parameters of the best-performing OFET devices, as well as the corresponding calculated average mobility. In particular, maximum field-effect mobilities of 0.78 and 0.41 $cm^2/(V\ s)$ were obtained for TIPS-PEN and diF-TES-ADT OFETs on glass, respectively. These mobility values were found to be at least 8 times higher than the maximum obtained in previously reported electrosprayed TIPS-PEN OFETs.[21,22] Most importantly, the proposed devices showed significantly improved V_T values (less than −5 V) and near-zero turn-on voltage (V_{on}), implying the sufficient switching behavior of the transistors.

Additionally, the I_{on}/I_{off} ratio was measured in the range from 10^4 to 10^5, while subthreshold slopes [SS = $\partial(\log I_{DS})/\partial V_{GS}$] of 1.48 and 2.27 V/dec were calculated for TIPS-PEN and diF-TES-ADT OFETs, respectively. The aforementioned switching characteristics represent indirect evidence of the good contact and interface quality between the semiconductor and dielectric.[42] Such an enhancement is mainly attributed to the presence of high-quality single-crystalline domains, which limit the detrimental effects of structural defects and grain boundaries to charge-carrier transport. To the best of our knowledge, these values are among the best obtained by spray-coated OFETs based on soluble acenes.[43−45] We should clarify though that the architecture of the fabricated transistors and/or the dielectric material in these reports may differ from our own.

Finally, top-contact OFETs were successfully fabricated on flexible substrates in order to demonstrate the scalability as well as adaptability of the ESD method with large-area technologies. Particularly, the transistors were integrated on heat-stabilized PET or PEN substrates, which are known to exhibit great dimensional and thermal stability, while a spin-coated layer of cPVP was used as the dielectric (Figure 6a,b). The deposition of the semiconducting layer was carried out using exactly the same process parameters as those described in the case of glass substrates. A mobility as high as 0.15 and 0.11 $cm^2/(V\ s)$ for the resulting flexible TIPS-PEN and diF-TES-ADT OFETs, respectively, was achieved, while both devices demonstrated relatively low threshold voltage values near (or less) than −5 V and on/off current ratios in the range of 10^3–10^4. Such a performance is comparable to that obtained in previously reported sprayed-coated flexible TIPS-PEN OFETs.[44]

These findings are of considerable importance given the fact that deposition of the semiconductor took place in ambient conditions and also that nonchlorinated solvents were employed for the sprayed solutions. Furthermore, investigation of the different characteristics of the various modes of ESD may reveal new approaches for the deposition of soluble organic semiconductors. For example, the microdripping mode, under certain conditions, could be used in a drop-on-demand operation, giving a great potential for the fabrication of reliable OFET arrays or organic integrated circuits.

Table 2. Electrical Parameters Obtained from the Best-Performing OFET Devices

substrate	semiconductor	μ_{max} [$cm^2/(V\ s)$]	V_T (V)	I_{on}/I_{off} ratio	SS (V/dec)	μ_{avg} [$cm^2/(V\ s)$]
glass	TIPS-PEN[a]	0.78	−2.8	7.9×10^4	1.6	0.47 ± 0.13
	diF-TES-ADT[a]	0.41	−1.9	2.1×10^4	2.2	0.26 ± 0.11
plastic	TIPS-PEN[b]	0.15	−5.3	3.0×10^3	3.2	0.095 ± 0.026
	diF-TES-ADT[b]	0.11	−2.6	2.8×10^3	4.0	0.092 ± 0.015

[a]The average mobility values calculated for 12 different OFET devices. [b]The average mobility values calculated for 6 different OFET devices.

DOI: 10.1021/am508162m
ACS Appl. Mater. Interfaces 2015, 7, 6496−6504

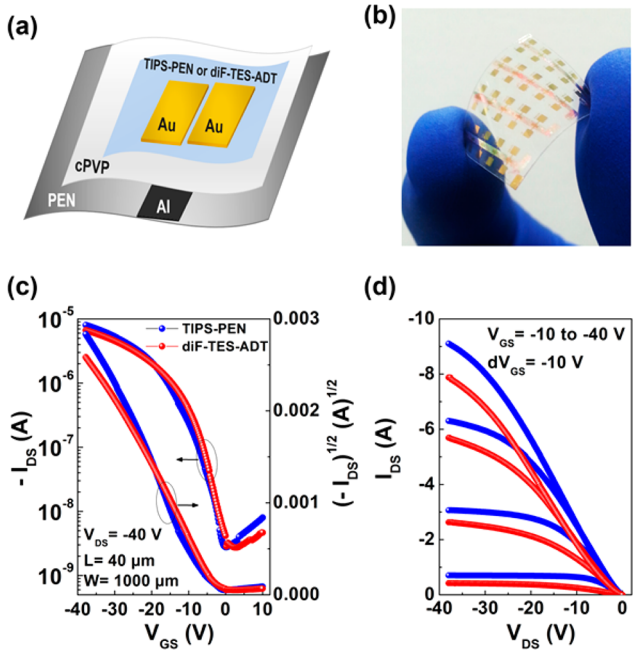

Figure 6. (a) Schematic representation of the device architecture and (b) optical image of OFETs fabricated on a plastic substrate. (c) Transfer and (d) output characteristics of electrospray-deposited TIPS-PEN- and diF-TES-ADT-based flexible OFETs. Devices had a top-contact/bottom-gate geometry, while their channel length and width were 40 and 1000 μm, respectively.

4. CONCLUSIONS

In summary, ESD was herein utilized for the deposition of soluble acenes toward the realization of high-performance OFETs. By optimization of the electrospraying regime as well as semiconducting solution properties, we successfully managed to obtain films with well-ordered crystalline domains and thus achieved a very competitive electrical performance. The fabricated OFET devices yielded excellent electrical characteristics, with high field-effect mobility up to 0.78 $cm^2/(V\ s)$, which is among the highest reported for sprayed OFETs, I_{on}/I_{off} $>10^4$, and near-zero threshold voltages. In a proof-of-concept study, flexible TIPS-PEN and dif-TES-ADT OFETs were realized using the optimized parameters. The presented results clearly demonstrated the feasibility and applicability of the proposed method and underlined its good potentiality as a versatile and effective large-area manufacturing process, offering a realistic view for roll-to-roll processing for flexible electronics.[46]

■ ASSOCIATED CONTENT

Supporting Information

AFM topographies and the corresponding roughness analysis of TIPS-PEN crystalline films for each different spraying regime and also information on the topography of a cPVP film spin-casted on glass and plastic substrates. This material is available free of charge via the Internet at http://pubs.acs.org.

■ AUTHOR INFORMATION

Corresponding Authors

*E-mail: cpitsali@physics.auth.gr.
*E-mail: logot@auth.gr.

Notes

The authors declare no competing financial interest.

■ ACKNOWLEDGMENTS

This work was partially supported by (a) the European Union (European Social Fund) and Greek national funds through the Operational Program "Education and Lifelong Learning" of the National Strategic Reference Framework Research Funding Program Heracleitus II and (b) EC Project REGPOT-286022 ROleMak.

■ REFERENCES

(1) Graham-Rowe, D. Electronic Paper Rewrites the Rulebook for Displays. *Nat. Photonics* **2007**, *1*, 248−251.
(2) Someya, T.; Kato, Y.; Sekitani, T.; Iba, S.; Noguchi, Y.; Murase, Y.; Kawaguchi, H.; Sakurai, T. Conformable, Flexible, Large-Area Networks of Pressure and Thermal Sensors with Organic Transistor Active Matrixes. *Proc. Natl. Acad. Sci. U. S. A.* **2005**, *102*, 12321−12325.
(3) Sekitani, T.; Yokota, T.; Zschieschang, U.; Klauk, H.; Bauer, S.; Takeuchi, K.; Takamiya, M.; Sakurai, T.; Someya, T. Organic Nonvolatile Memory Transistors for Flexible Sensor Arrays. *Science* **2009**, *326*, 1516−1519.
(4) Mannsfeld, S.; Tee, B. Highly Sensitive Flexible Pressure Sensors with Microstructured Rubber Dielectric Layers. *Nat. Mater.* **2010**, *9*, 859−864.
(5) Ito, Y.; Virkar, A. A.; Mannsfeld, S.; Oh, J. H.; Toney, M.; Locklin, J.; Bao, Z. Crystalline Ultrasmooth Self-Assembled Monolayers of Alkylsilanes for Organic Field-Effect Transistors. *J. Am. Chem. Soc.* **2009**, *131*, 9396−9404.
(6) Minemawari, H.; Yamada, T.; Matsui, H.; Tsutsumi, J.; Haas, S.; Chiba, R.; Kumai, R.; Hasegawa, T. Inkjet Printing of Single-Crystal Films. *Nature* **2011**, *475*, 364−367.
(7) Smith, J.; Zhang, W.; Sougrat, R.; Zhao, K.; Li, R.; Cha, D.; Amassian, A.; Heeney, M.; McCulloch, I.; Anthopoulos, T. D. Solution-Processed Small Molecule-Polymer Blend Organic Thin-Film Transistors with Hole Mobility Greater than 5 cm^2/Vs. *Adv. Mater.* **2012**, *24*, 2441−2446.
(8) Diao, Y.; Tee, B. C.-K.; Giri, G.; Xu, J.; Kim, D. H.; Becerril, H. A.; Stoltenberg, R. M.; Lee, T. H.; Xue, G.; Mannsfeld, S. C. B.; Bao, Z. Solution Coating of Large-Area Organic Semiconductor Thin Films with Aligned Single-Crystalline Domains. *Nat. Mater.* **2013**, *12*, 665−671.
(9) Tszydel, I.; Kucinska, M.; Marszalek, T.; Rybakiewicz, R.; Nosal, A.; Jung, J.; Gazicki-Lipman, M.; Pitsalidis, C.; Gravalidis, C.; Logothetidis, S.; Zagorska, M.; Ulanski, J. High-Mobility and Low Turn-On Voltage N-Channel OTFTs Based on a Solution-Processable Derivative of Naphthalene Bisimide. *Adv. Funct. Mater.* **2012**, *22*, 3840−3844.
(10) Anthony, J. E.; Brooks, J. S.; Eaton, D. L.; Parkin, S. R. Functionalized Pentacene: Improved Electronic Properties from Control of Solid-State Order. *J. Am. Chem. Soc.* **2001**, *123*, 9482−9483.
(11) Subramanian, S.; Park, S. K.; Parkin, S. R.; Podzorov, V.; Jackson, T. N.; Anthony, J. E. Chromophore Fluorination Enhances Crystallization and Stability of Soluble Anthradithiophene Semiconductors. *J. Am. Chem. Soc.* **2008**, *130*, 2706−2707.
(12) Shcherbyna, S. V.; Bohme, D. K.; Baranov, V. I.; Loboda, A.; Swartz, C. R.; Anthony, J. E. Clustering of Pentacene and Functionalized Pentacene Ions in a Matrix-Assisted Laser Desorption/ionization Orthogonal TOF Mass Spectrometer. *J. Am. Soc. Mass Spectrom.* **2006**, *17*, 222−229.
(13) Park, S. K.; Mourey, D. A.; Han, J.-I.; Anthony, J. E.; Jackson, T. N. Environmental and Operational Stability of Solution-Processed 6,13-Bis(triisopropyl-silylethynyl) Pentacene Thin Film Transistors. *Org. Electron.* **2009**, *10*, 486−490.
(14) Choi, D.; Ahn, B.; Kim, S. H.; Hong, K.; Ree, M.; Park, C. E. High-Performance Triisopropylsilylethynyl Pentacene Transistors via Spin Coating with a Crystallization-Assisting Layer. *ACS Appl. Mater. Interfaces* **2012**, *4*, 117−122.
(15) Pitsalidis, C.; Kalfagiannis, N.; Hastas, N. A.; Karagiannidis, P. G.; Kapnopoulos, C.; Ioakeimidis, A.; Logothetidis, S. High Perform-

DOI: 10.1021/am508162m
ACS Appl. Mater. Interfaces 2015, 7, 6496−6504

ance Transistors Based on the Controlled Growth of Triisopropylsilylethynyl-Pentacene Crystals via Non-Isotropic Solvent Evaporation. *RSC Adv.* **2014**, *4*, 20804.
(16) Cho, S. Y.; Ko, J. M.; Lim, J.; Lee, J. Y.; Lee, C. Inkjet-Printed Organic Thin Film Transistors Based on TIPS Pentacene with Insulating Polymers. *J. Mater. Chem. C* **2013**, *1*, 914.
(17) Zhao, X.-Y.; Wang, X.; Lim, S. L.; Qi, D.; Wang, R.; Gao, Z.; Mi, B.; Chen, Z.-K.; Huang, W.; Deng, W. Enhancement of the Performance of Organic Solar Cells by Electrospray Deposition with Optimal Solvent System. *Sol. Energy Mater. Sol. Cells* **2014**, *121*, 119−125.
(18) Ju, J.; Yamagata, Y.; Higuchi, T. Thin-Film Fabrication Method for Organic Light-Emitting Diodes Using Electrospray Deposition. *Adv. Mater.* **2009**, *21*, 4343−4347.
(19) Khan, S.; Doh, Y. H.; Khan, A.; Rahman, A.; Choi, K. H.; Kim, D. S. Direct Patterning and Electrospray Deposition through EHD for Fabrication of Printed Thin Film Transistors. *Curr. Appl. Phys.* **2011**, *11*, S271−S279.
(20) Kim, Y.; Lee, J.; Kang, H.; Kim, G.; Kim, N.; Lee, K. Controlled Electro-Spray Deposition of Highly Conductive PEDOT:PSS Films. *Sol. Energy Mater. Sol. Cells* **2012**, *98*, 39−45.
(21) Onojima, N.; Saito, H.; Kato, T. Bottom-Contact Organic Field-Effect Transistors Based on Single-Crystalline Domains of 6,13-Bis(triisopropylsilylethynyl) Pentacene Prepared by Electrostatic Spray Deposition. *Org. Electron.* **2013**, *14*, 2406−2410.
(22) Yamauchi, H.; Sakai, M.; Kuniyoshi, S.; Kudo, K. Fabrication of N- and P-Channel Step-Edge Vertical-Channel Transistors by Electrospray Deposition. *Jpn. J. Appl. Phys.* **2014**, *53*, 01AB16.
(23) Jaworek, A.; Sobczyk, A. T. Electrospraying Route to Nanotechnology: An Overview. *J. Electrost.* **2008**, *66*, 197−219.
(24) Almería, B.; Deng, W.; Fahmy, T. M.; Gomez, A. Controlling the Morphology of Electrospray-Generated PLGA Microparticles for Drug Delivery. *J. Colloid Interface Sci.* **2010**, *343*, 125−133.
(25) Hayati, I.; Bailey, A.; Tadros, T. Investigations into the Mechanisms of Electrohydrodynamic Spraying of Liquids. *J. Colloid Interface Sci.* **1987**, *117*, 205−221.
(26) Onojima, N.; Takahashi, S.; Kato, T. Pentacene-Based Organic Field-Effect Transistors with Poly(methyl methacrylate) Top-Gate Insulators Fabricated by Electrostatic Spray Deposition. *Synth. Met.* **2013**, *177*, 72−76.
(27) Wo, S.; Headrick, R. L.; Anthony, J. E. Fabrication and Characterization of Controllable Grain Boundary Arrays in Solution-Processed Small Molecule Organic Semiconductor Films. *J. Appl. Phys.* **2012**, *111*, 073716.
(28) Choi, D.; Jin, S.; Lee, Y.; Kim, S. H.; Chung, D. S.; Hong, K.; Yang, C.; Jung, J.; Kim, J. K.; Ree, M.; Park, C. E. Direct Observation of Interfacial Morphology in Poly(3-Hexylthiophene) Transistors: Relationship between Grain Boundary and Field-Effect Mobility. *ACS Appl. Mater. Interfaces* **2010**, *2*, 48−53.
(29) De Gans, B.-J.; Schubert, U. S. Inkjet Printing of Well-Defined Polymer Dots and Arrays. *Langmuir* **2004**, *20*, 7789−7793.
(30) Lim, J.; Lee, W.; Kwak, D.; Cho, K. Evaporation-Induced Self-Organization of Inkjet-Printed Organic Semiconductors on Surface-Modified Dielectrics for High-Performance Organic Transistors. *Langmuir* **2009**, *25*, 5404−5410.
(31) Cloupeau, M.; Prunet-Foch, B. Electrostatic Spraying of Liquids: Main Functioning Modes. *J. Electrost.* **1990**, *25*, 165−184.
(32) Nemes, P.; Marginean, I.; Vertes, A. Spraying Mode Effect on Droplet Formation and Ion Chemistry in Electrosprays. *Anal. Chem.* **2007**, *79*, 3105−3116.
(33) Jadhav, A.; Wang, L.; Padhye, R. Influence of Applied Voltage on Droplet Size Distribution in Electrospraying of Thermoplastic Polyurethane. *Int. J. Mater. Mech. Manuf.* **2013**, *1*, 287−289.
(34) Marginean, I.; Nemes, P.; Vertes, A. Order−Chaos−Order Transitions in Electrosprays: The Electrified Dripping Faucet. *Phys. Rev. Lett.* **2006**, *064502*, 1−4.
(35) Speranza, A.; Ghadiri, M.; Newman, M.; Osseo, L. S.; Ferrari, G. Electro-Spraying of a Highly Conductive and Viscous Liquid. *J. Electrost.* **2001**, *51−52*, 494−501.
(36) Teague, L. C.; Hamadani, B. H.; Jurchescu, O. D.; Subramanian, S.; Anthony, J. E.; Jackson, T. N.; Richter, C. A.; Gundlach, D. J.; Kushmerick, J. G. Surface Potential Imaging of Solution Processable Acene-Based Thin Film Transistors. *Adv. Mater.* **2008**, *20*, 4513−4516.
(37) Radacsi, N.; Stankiewicz, A. I.; Creyghton, Y. L. M.; van der Heijden, A. E. D. M.; ter Horst, J. H. Electrospray Crystallization for High-Quality Submicron-Sized Crystals. *Chem. Eng. Technol.* **2011**, *34*, 624−630.
(38) Akkerman, H. B.; Chang, A. C.; Verploegen, E.; Bettinger, C. J.; Toney, M. F.; Bao, Z. Fabrication of Organic Semiconductor Crystalline Thin Films and Crystals from Solution by Confined Crystallization. *Org. Electron.* **2012**, *13*, 235−243.
(39) Jang, J.; Nam, S.; Im, K.; Hur, J.; Cha, S. N.; Kim, J.; Son, H.; Suh, H.; Loth, M. A.; Anthony, J. E.; Park, J.-J.; Park, C. E.; Kim, J. M.; Kim, K. Highly Crystalline Soluble Acene Crystal Arrays for Organic Transistors: Mechanism of Crystal Growth during Dip-Coating. *Adv. Funct. Mater.* **2012**, *22*, 1005−1014.
(40) Boudinet, D.; Benwadih, M.; Altazin, S.; Gwoziecki, R.; Verilhac, J. M.; Coppard, R.; Le Blevennec, G.; Chartier, I.; Horowitz, G. Influence of the Semi-Conductor Layer Thickness on Electrical Performance of Staggered N- and P-Channel Organic Thin-Film Transistors. *Org. Electron.* **2010**, *11*, 291−298.
(41) Sohn, C.; Rim, T. Analysis of Contact Effects in Inverted-Staggered Organic Thin-Film Transistors Based on Anisotropic Conduction. *IEEE Trans. Electron Devices* **2010**, *57*, 986−994.
(42) Li, X.; Kjellander, B. K. C.; Anthony, J. E.; Bastiaansen, C. W. M.; Broer, D. J.; Gelinck, G. H. Azeotropic Binary Solvent Mixtures for Preparation of Organic Single Crystals. *Adv. Funct. Mater.* **2009**, *19*, 3610−3617.
(43) Owen, J. W.; Azarova, N. A.; Loth, M. A.; Paradinas, M.; Coll, M.; Ocal, C.; Anthony, J. E.; Jurchescu, O. D. Effect of Processing Parameters on Performance of Spray-Deposited Organic Thin-Film Transistors. *J. Nanotechnol.* **2011**, *2011*, 1−6.
(44) Shao, M.; Das, S.; Xiao, K.; Chen, J.; Keum, J. K.; Ivanov, I. N.; Gu, G.; Durant, W.; Li, D.; Geohegan, D. B. High-Performance Organic Field-Effect Transistors with Dielectric and Active Layers Printed Sequentially by Ultrasonic Spraying. *J. Mater. Chem. C* **2013**, *1*, 4384.
(45) Azarova, N. A.; Owen, J. W.; McLellan, C. A.; Grimminger, M. A.; Chapman, E. K.; Anthony, J. E.; Jurchescu, O. D. Fabrication of Organic Thin-Film Transistors by Spray-Deposition for Low-Cost, Large-Area Electronics. *Org. Electron. Phys., Mater. Appl.* **2010**, *11*, 1960−1965.
(46) Logothetidis, S. Flexible Organic Electronic Devices: Materials, Process and Applications. *Mater. Sci. Eng., B* **2008**, *152*, 96−104.

DOI: 10.1021/am508162m
ACS Appl. Mater. Interfaces 2015, 7, 6496−6504